

Synthesis of Nano sized Ce-Co Doped Zinc Ferrite and their Permittivity and Hysteresis Studies.

K.Muthuraman
Dept of Chemistry
Sethu Inst. of Tech.,
Pulloor – 626115,
Tamilnadu, India

S. Alagarsamy
Dept of ECE
Sethu Inst. of Tech.,
Pulloor – 626115,
Tamilnadu, India

M. Ameena Banu
Dept of ECE . Sethu
Inst. of Tech., Pulloor
– 626115, Tamilnadu,
India,

Vasant Naidu
Dept of ECE
Sethu Inst. of Technology,
Pulloor – 626115,
Tamilnadu, India

ABSTRACT:

The effect of Cerium and Cobalt substitution in Zinc ferrites with respect to their electrical and magnetic properties has been investigated in this paper. The nanoparticles of $Zn_{1-x-y}Ce_xCo_yFe_2O_4$ ($x = 0.012, 0.014, 0.016, 0.018$; $y = 0.01, 0.001, 0.014, 0.016$) is prepared by sol gel route and sintered in a microwave furnace. The nano size, structure and composition of Ce-Co doped Zinc ferrite ceramics are analyzed by X-ray diffraction and further confirmed by SEM monographs, FTIR, and EDAX. By analyzing the change in magnetic saturation and coercivity, the magnetic behaviour of these nano ferrite materials is confirmed. The electrical measurements have been performed to determine the dielectric constant (ϵ_r), dielectric loss (ϵ_r') and loss tangent in the frequency range of 20KHz - 20MHz. It is also found that the permittivity of these nano materials is being reduced with the increase in frequency.

Keywords: Nano ferrite materials; Sol gel, cerium doped, VSM, SEM, EDAX, Permittivity Studies

1. INTRODUCTION

Nano ferrites material has applications in making high density information storage[1], chlorine gas sensors[2], color imaging[3], cores of audio frequency and high frequency transformers coils,

magneto optical displays, electromagnetic wave absorption[4], microwave absorbers, wave guides in the GHz region[2], medical diagnosis[5] and many more. The Multi layer chip inductor (MLCI) has been recently developed as a key surface mounting device [5]. Magnetic particles with sizes in the nanometer scale are now of interest because of their many technological applications and unique magnetic properties which differ considerably from those of bulk materials. Below a critical size, magnetic particles become single domain in contrast with the usual multi domain structure of the bulk magnetic materials, thus exhibiting unique phenomena such as super paramagnetic and quantum tunneling of the magnetization[6]. Magnetic nano particle systems exhibiting super paramagnetic behavior, display little or no remanence and coercivity while keeping a very high saturation magnetization. It is seen that they have a lot of potential application in magnetic drug delivery, biomedicine and cell-sorting systems [7-9]. It is well known that low temperature sintering ferrites can be achieved by using ultra fine particles powders synthesized via sol gel route [10-11] and sintered in the microwave furnace [11].

The spinel cobalt zinc ferrite $Co_xZn_xFe_{2-x}O_4$ plays an important role in microwave absorbing materials over a wide range of frequencies starting from a few hundred hertz to several Megahertz, because of their remarkable properties which are obtained in the

bulk sample with high saturation magnetization, high coercivity, strong anisotropy along with good mechanical hardness and chemical stability. The high permeability and high electrical resistivity in this frequency range make them particularly useful for inductor and transformer cores as well as in switch mode power supplies (SMPS) [12]. Many physical properties of these polycrystalline ferrites are very sensitive to their microstructure. The bulk (grain) and grain boundary are the two main components that are used to determine the microstructure. Thus, these information is about associated physical parameters of the components are important in understanding the overall behaviour of these materials.

The purpose of our present work is to prepare the nano sized Ce-Co doped Zinc ferrite and to study its structural property. Further the studies are extended for the determination of dielectric constant, dielectric loss and magnetic property for practical application particularly for the design and the construction of patch antenna.

2. EXPERIMENTAL PROCEDURE

2.1 Synthesis Technique:

The nano sized Zinc ferrite doped with different concentration of Cerium(Ce) and Cobalt(Co) is prepared by using the AR grade nitrates of Co(Merck) ,Zinc(Alfa Aesar) and ferric(Lobo Chem) and rare earth Ce(Alfa Aesar), along with citric acid(Merck) in a certain molar ratio of 1:1 and then dissolved in deionized water, here the citric acid helps the homogenous distribution of the metal ions to get segregate from the solutions. Further a required amount of ammonia is added in order to adjust the pH value to about 7, since the base catalysts are employed in order to speed up the reaction. The solution is later subjected to a continuous stirring for duration of 24 hrs. This as prepared solution is heated to a constant temperature of 135°C to condense it into a xerogel [11-12]. After this dehydration process a brown colored dried gel is obtained. The burnt powder is further crushed in agate mortar to obtain the nano

sized powder. Further the powder is subjected to sintering in a microwave furnace.

The grain size of the nanoferrite is determined from the prominent peak of XRD using Scherer's equation. Using the knowledge of site preference of the ions and the ionic size data of the respective ions, the cation distribution has been estimated theoretically using the formula as proposed [13, 14]. These nano ferrites possess a very well defined local atomic ordering that may be described in terms of a spinel-type structure with Zn^{2+} and Fe^{3+} ions which is almost randomly distributed over its tetrahedral and octahedral sites. The new structural information helps to explain the material's unusual magnetic properties [15]. The experimental magnetic moment is calculated from the following formula [16].

$$\eta = \frac{[M_W * M_S]}{5585}$$

Where M_W is the molecular weight of the sample and M_S is the saturation magnetization in emu/g.

2.2 XRD and EDX Studies

The phase composition of fine ferrite powder is carried out using PAN analytical X'pert PRO diffraction meter using $Cu K_{\alpha}$ radiation ($\lambda=1.54\text{\AA}$) at 40KV and 30mA with a scanning rate of $0.01^\circ/s$ and scan speed of $1^\circ/min$ in a 2θ range of $10-80^\circ\text{A}$. The crystallite size is calculated by taking RWHM of the 1,1,1 peak in XRD and using the Scherrer formula. The energy dispersive studies (EDAX) are done on Genesis EDAX to confirm the presence of chemical composition of the powder and to study the structure of the powdered material and the presence of the elements.

2.3 FTIR Analysis

The Infrared absorption spectra are found to be in the range of $3.72 \times 10^4 \text{ m}^{-1}$ to $5.41 \times 10^4 \text{ m}^{-1}$, they are recorded at room temperature by using SHIMADZU.FTIR spectrum using KBr pellet method. From the FTIR studies with respect to the spectrum transmittance (%) against wave number (m^{-1}) is used for interpretation of the results.

2.4 SEM Studies

SEM Micrographs of the nanoferrite powder are recorded using the scanning electron microscope (HITACHI model S-3000H).

2.5 Magnetic Measurements

The Magnetic measurements are performed on the commercial vibrating sample magnetometer (VSM) Lakeshore (Model73009). The Magnetic hysteresis loops are measured at the room temperature with maximal applied magnetic fields up to 0.95T. Magnetic field sweep rate is kept at 5 Oe/s for all the measurements, so that the measurement of hysteresis loops with maximum field of 0.989 T is taken from an interval of three hours. The saturation magnetization, coercivity and remanent magnetization are found from hysteresis loop.

2.6 Electrical Measurements

The Electrical measurements are performed using the N4L LCR meter. The experimental set up for measuring the dielectric properties in the microwave region consisted of a pallet holder connected to the N4L LCR meter interfacing the computer. The microwave properties of the four samples Ce_xCo_y doped zinc ferrite $x = 0.012, 0.014, 0.016, 0.018$; $y = 0.01, 0.001, 0.014, 0.016$ are investigated at the frequency range from 20 KHz to 20 MHz. The electrical conduction mechanism can be explained by the electron hopping model of Heikes and Johnston [17].

3. RESULT AND DISCUSSION:

3.1 X-RAY DIFFRACTION

A careful analysis of the XRD patterns helps to determine the respective planes and face centered cubic structure of these ferrites. Well resolved peaks in XRD pattern clearly indicates the single phase and polycrystalline nature of the samples.

Figure 1 shows XRD patterns of the $\text{Zn}_{1-x-y}\text{Ce}_x\text{Co}_y\text{Fe}_2\text{O}_4$ powders. The diffraction patterns and relative intensities of all diffraction peaks are matched well

with those of JCPDS card 22-1086 for $\text{Co}_{0.5}\text{Zn}_{0.5}\text{Fe}_2\text{O}_4$ and the Ce diffraction peaks are matched well with those of JCPDS card 34-0394. The peaks are appeared at around $18.5^\circ, 30.2^\circ, 35.6^\circ, 37.2^\circ$ and 43.0° for Co and Ce, 53.4° for Ce and $57.1^\circ, 62.5^\circ$ and 73.7° appeared for Co. These peaks are well indexed to the crystal plane of spinel ferrite (111), (220), (311), (222), (400), (422), (511), (440) and (533), respectively. The diffraction peaks are quite sharp because of the micrometer size of the crystallite. XRD patterns clearly indicate that the pure CoFe_2O_4 shows the presence of single-phase cubic spinel structure. The X-ray diffraction patterns show that all samples are formed in cubic single spinel phase. No foreign impurity lines are seen. The lattice parameter a (Å) is calculated using Bragg's law.

Where h, k, l are the indices of mentioned planes. Lattice constants of all samples that are prepared in investigation are listed in Table 1. The lattice constants of individual phases do not vary much by the inclusion of Co- Ce and it was found that the porosity and density had shown an increase with increase in Co- Ce doping concentration.

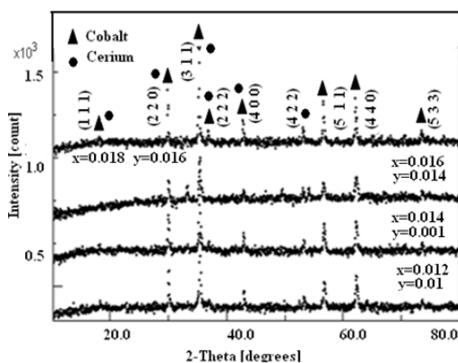


Fig1 XRD patterns of sintered $\text{Zn}_{1-x-y}\text{Ce}_x\text{Co}_y\text{Fe}_2\text{O}_4$ $x=0.012, 0.014, 0.016, 0.018$

Table 1 Lattice parameter (a), crystallite size (D), X-ray density (d_x), porosity (p) and observed molar contents of $\text{Zn}_{1-x-y}\text{Ce}_x\text{Co}_y\text{Fe}_2\text{O}_4$

| Zn _{1-x-y} Ce _x Co _y Fe ₂ O ₄ | x=0.012 y=0.01 | x=0.014 y=0.001 | x=0.016 y=0.014 | x=0.018 y=0.016 |
|---|-------------------|--------------------|--------------------|--------------------|
| a(A°) | 8.424 | 8.45 | 8.43 | 8.424 |
| D(nm) | 41.52 | 70.28 | 28.36 | 41.63 |
| d _x x10 ³ gcm-3 | 3.456 | 3.687 | 3.948 | 4.239 |
| p | 0.342 | 0.385 | 0.405 | 0.460 |
| Observed contents (Co) | 0.012 | 0.014 | 0.016 | 0.018 |
| Observed Contents (Ce) | 0.01 | 0.001 | 0.014 | 0.016 |
| (±0.01 mol) Fe | 1.978 | 1.985 | 1.97 | 1.964 |

The size of crystal is evaluated by measuring the FWHM of the most intense peak (311) from XRD and by using the Debye Scherrer's formula [18], the size of the crystal is evaluated.

$$D = \frac{0.94\lambda}{\beta \cos\theta}$$

Here the XRD patterns exhibit narrow reflection that points out the narrow size crystallites. The mean crystallite size of the sample lies within the range of 28.37nm to 70.28nm. The lattice parameter shows an increases for x = 0.012 composition and then starts decreasing for x=0.014, 0.016 composition.

3.3 EDAX

The EDAX spectra (Fig.2 and Fig 3) obtained from the center of Ce-Co substituted Zinc ferrite grains indicated the presence of Zn peaks at 8.2 - 9.7keV, where as Ce grains are seen in between the energy range of 4keV and 6keV, Co grains are seen in between 6.5keV and 8keV and the Fe peaks are seen at 6.2keV and 6.7ke. These observations conclude that most of the Co and Ce grains are attached to Zn.

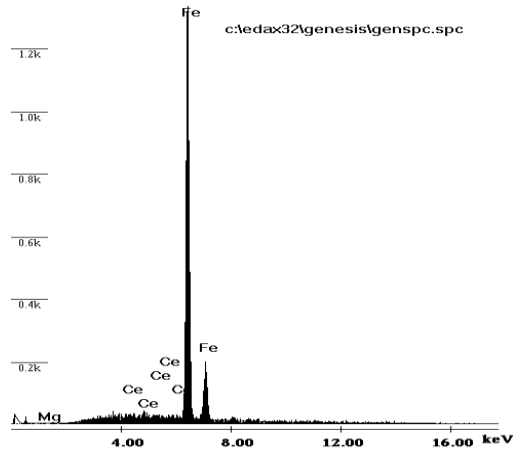


Fig.2 EDAX pattern for Zn_{1-x-y} Ce_x Co_y Fe₂O₄ x=0.012,0.01

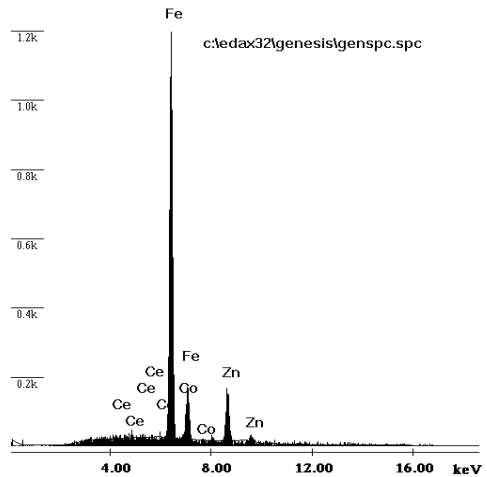


Fig.3 EDAX pattern for Zn_{1-x-y} Ce_x Co_y Fe₂O₄ x=0.016,0.014

3.2 SEM analysis

The nano phase is investigated by using the SEM micrograph, as shown in Fig. they show the microstructure of the sintered specimen. These Ce-

doped specimens show a bi-phasic microstructure constituted of dark ferrite matrix grains and small whitish grain at the grain junction/boundary. As proposed by Sattar et, al [19] the rare earth ions occupy either the iron positions or go to the grain boundaries. However, we have to exclude the probability that the rare earth ions occupy the A site of Fe^{3+} ions. This is due to the fact that the tetrahedral sites are small to be occupied by the large rare earth ions which have large ionic radius.

Of course the probability of occupancy of the octahedral (B-site) is by the rare earth ions (Ce). With the increase in Ce ions the ionic radius R decreases. This is indicated by the whitish grains of Ce-Co with Fe_2O_4 . The amount of Ce-Co with Fe_2O_4 is maximum in $x = 0.016$ composition. The grain size of matrix phase is also maximum in $x = 0.016$ composition. Relatively lower grain size of ferrite matrix is seen in $x= 0.012$ compositions, it may be due to the grain growth inhibition caused by $Ce Fe_2O_4$.

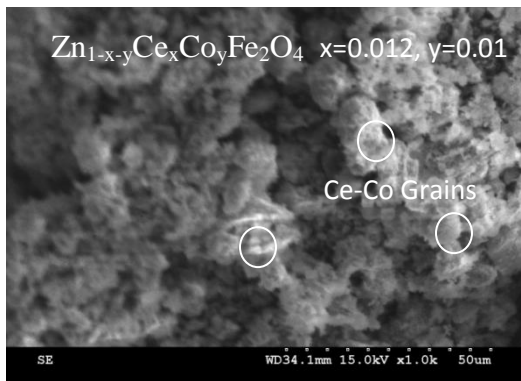


Fig.4 $Zn_{1-x-y}Ce_xCo_yFe_2O_4$ $x=0.012, y=0.01$

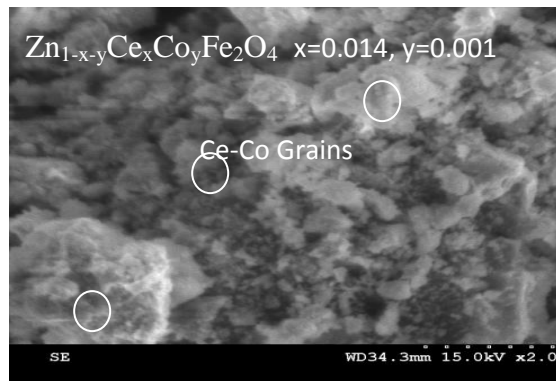


Fig.5 $Zn_{1-x-y}Ce_xCo_yFe_2O_4$ $x=0.014, y=0.001$



Fig.6 $Zn_{1-x-y}Ce_xCo_yFe_2O_4$ $x=0.016, y=0.014$



Fig.7 $Zn_{1-x-y}Ce_xCo_yFe_2O_4$ $x=0.018, y=0.016$

3.4. FTIR study

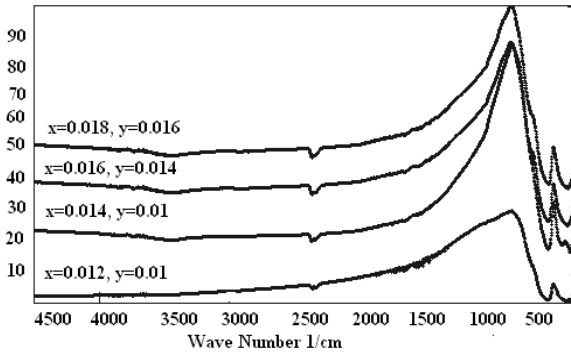


Fig.8 FTIR absorption spectra of the samples

The study of far-infrared spectra is an important tool to get the information about the position of ions in the crystal [20]. FTIR absorption spectra of the samples of the high and low frequency absorption bands (ν_1 , ν_2) at the range of $376.09 \times 10^4 \text{ m}^{-1}$ to $541.96 \times 10^4 \text{ m}^{-1}$ are given in Fig. 8. The spectra shows two major absorption bands in this given frequency range mentioned in Table 2, which is attributed to tetrahedral and octahedral complexes $\text{Fe}^{3+}-\text{O}^{2-}$. These two bands have been reported by Waldron [21] in spinel structure of ferrite, the shift of absorption band ν_1 and ν_2 is observed. The absorption band ν_1 and ν_2 is slightly shifted to upper frequency side with addition of R ions and is attributed to increase in bond length on the B-site [22-23]. This suggests that the rare-earth ions occupy the B-site. The difference in frequencies between ν_1 and ν_2 is due to changes in bond length ($\text{Fe}^{3+}-\text{O}^{2-}$) at tetrahedral and octahedral sites [24]. The broadening of the ν_2 band is observed in rare-earth added MgFe_2O_4 , which suggests the occupancy of rare-earth ions on the B-sites [24].

The inter-ionic separation may face an extension due to less number of structural matters in the

surrounding of each nano particle. Thus the nano size of the ferrite particles and ultimate change of

| $\text{Zn}_{1-x-y}\text{Ce}_x\text{Co}_y\text{Fe}_2\text{O}_4$ | | Absorption/ cm^{-1} | |
|--|-------|------------------------------|---------|
| x | y | ν_1 | ν_2 |
| 0.012 | 0.01 | 541.96 | 385.74 |
| 0.014 | 0.001 | 540.03 | 391.52 |
| 0.016 | 0.014 | 541.96 | 372.24 |
| 0.018 | 0.016 | 541.96 | 376.09 |

Table 2. FTIR to show the rare-earth ions occupation in the B-site

the nature of ions in the respective size can be a cause for reduction of magnetization in MgFe_2O_4 . Thus in nano regime, the magnetization is said to be dependent on grain size and cation distribution. Table 2 shows the changes in ν_1 and ν_2 . The value of change in the difference Cobalt and Cerium, which leads into the change in retentivity and change in coercive force of frequency increase with the increase in the values of Cobalt and Cerium in zinc ferrite

. The grains in the unsubstituted sample are inhomogeneous i.e., the grains are affected by certain stress, while the grains for the Fe substituted sample are nearly homogeneous due to the decrease of stress. The photographs confirm these results that the stability has increased for the substituted samples.

3.5 Hysteresis studies:

The different parameters such as saturation magnetization (M_C), coercive force (H_C), and

Retentivity, The dielectric constant ϵ_r and dielectric

microwave frequency range from 10M–20GHz are

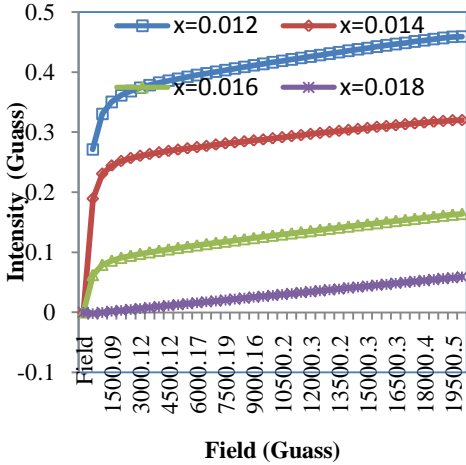


Fig 9 Saturation magnetization of $Zn_{1-x-y}Ce_xCo_yFe_2O_4$

| $Zn_{1-x-y}Ce_xCo_yFe_2O_4$ | | M_s (emu) | Coercivity (G) | Retentivity (emu)X10 ⁻³ | ϵ_r | ϵ_r' |
|-----------------------------|-------|-------------|----------------|------------------------------------|--------------|---------------|
| x | y | | | | | |
| 0.012 | 0.01 | 0.067 | 70.858 | 6.5083 | 3.8 | 4.37 |
| 0.014 | 0.001 | 0.113 | 156.39 | 2.8380 | 0.65 | 0.56 |
| 0.016 | 0.014 | 0.132 | 189.39 | 9.9111 | 2.25 | 2.32 |
| 0.018 | 0.016 | 0.157 | 204.48 | 7.5684 | 2.69 | 2.99 |

Table 3 The change in magnetic saturation, retentivity, coercive force, relative permittivity ϵ_r (at frequency GHz) and absolute permittivity (ϵ_r') (at frequency GHz) with change in Ce-Co concentration respectively.

loss ϵ_r' are listed in Table 3. The magnetic properties have been seen to be altered by the

addition of Co and Ce in Zn ferrite, It is observed that the saturation magnetization increases with the addition of Co and Ce. Rezlescu et al. [24], the saturation magnetization of Ce^{3+} and Co^{3+} is substituted in Zn ferrites is higher than that of un substituted ferrite. Similar results are reported by Liu et al. [25] in Co^{3+} substituted M-type Cerium ferrite and similar results is reported by Gama et al is seen in cerium-doped Zn ferrite [26]. Therefore 3.8 is observed for the sample $Zn_{0.978}Ce_{0.012}Co_{0.01}Fe_2O_4$ and minimum is 0.645 for the sample $Zn_{0.985}Ce_{0.014}Co_{0.001}Fe_2O_4$, as mentioned in table 3. These values are attributed to better concentration and nature of the ions in A and B site causes resultant magnetization to be different as reported.

3.6 Electrical Properties

The dielectric constant ϵ_r and dielectric loss ϵ_r' of the sintered samples $ZnCe_xCo_yFe_{2-x-y}O_4$, over the

shown in figure 10 and 11. The plots 11,12 show that the ϵ_r and ϵ_r' values tend to decrease exponentially, it is also seen that the value of ϵ_r and ϵ_r' increases with the addition of Cerium and Cobalt atom concentration, while the capacitance value remains fairly constant over the frequency range of study. The maximum value of dielectric constant compositional stoichiometry single phase spinel structure and uniform microstructure of the sample. The general trend for all composition is that ϵ and ϵ'' decrease with increasing frequency. single phase spinel structure and uniform microstructure of the sample. The general trend for all composition is that ϵ and ϵ'' decrease with increasing frequency.

This behavior of a dielectric may be explained qualitatively by the supposition that the mechanism of the polarization process in ferrite is similar to that the conduction process. e_2O_4 , as mentioned in table 3. These values are attributed to better compositional stoichiometry single phase spinel structure and uniform microstructure of the sample. The general trend for all composition is that ϵ and ϵ'' decrease with increasing frequency. This behavior of a dielectric may be explained qualitatively by the

supposition that the mechanism of the polarization process in ferrite is similar to that the conduction process. The electrical conduction mechanism can be explained by the electron hopping model of Heikes and Johnston [17]. It is known that the effect

of polarization is to reduce the field inside the medium. Therefore, the dielectric constant of a substance may be decreased substantially as the frequency is increased.

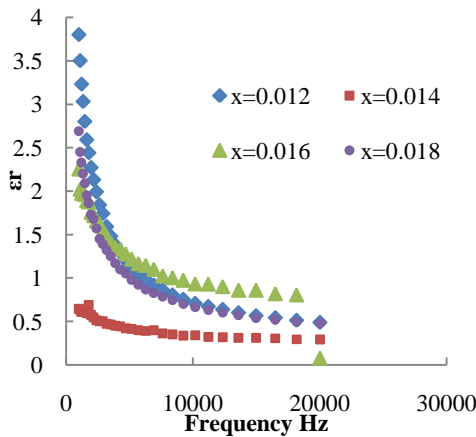


Fig10.Dielectric constant for $Zn_{1-x-y}Ce_xCo_yFe_2O_4$

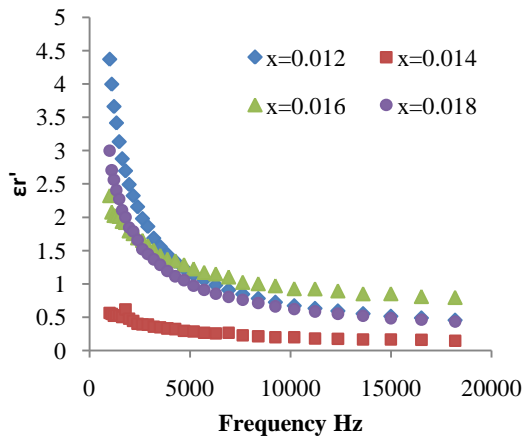


Fig 11. Dielectric loss for $Zn_{1-x-y}Ce_xCo_yFe_2O_4$

4. CONCLUSION:

The dielectric constant ϵ_r and the dielectric loss ϵ_r'' decrease with increasing frequency for all $Zn_{1-x-y}Ce_xCo_yFe_2O_4$ compositions. This behavior of a dielectric is explained qualitatively in terms of the supposition that the process of dielectric polarization takes place through a mechanism similar to the conduction process. The increase in the electrical conductivity at low temperature is attributed to the impurities, which reside at the grain boundaries. It is seen that the value of ϵ_r and ϵ_r'' increases with the addition of Cerium and Cobalt atom concentration, while the capacitance value remains fairly constant for this range of frequency. This investigation also indicates that the addition of Cobalt and Cerium in zinc ferrite showed a small change in magnetic properties. It is expected that a large concentration of Cerium and Cobalt may cause a significant structural change which in turn may enhance the magnetic properties [27-28].

5. REFERENCES

- [1] R.F. Zolio, US patent 4, 474 (1984) 866
- [2] C V Gopal Reddy, S V Manorama, and V J Rao., semiconducting gas sensor for chlorine based on inverse spinel Nickel ferrite., *Sensors and Actuators B*, 1999,55(1), 90-95.
- [3] L Nixon., C. A Koval., R.D Noble., G.S Slaff., Preparation and characterization of novel magnetic coated ion exchange particles, *Chem. Mater.*,1992,4,117
- [4] S.N. Dolia, Role of Particle Size on Structural and Magnetic Behavior of Nanocrystalline Cu-Ni Ferrite, *Solid State Phenomena* ,2011, 171 79-91.

- [5] P.K. Roy and J. Bera., Enhancement of the magnetic properties of Ni–Cu–Zn ferrites with the substitution of a small fraction of lanthanum for iron, Published in Materials Research Bulletin (2006)
- [6] Y L N Murthy, I V Kasi Viswanath, T. Kondala Rao, Rajendra singh., Synthesis and characterization of Nickel Copper Ferrite, International Journal of ChemTech Research 2009 ,Vol.1, No.4, pp 1308-1311.
- [7] Ruuge J.K., Ruzetski A.N., Magnetic fluids as drug carriers: Targetted transport of drugs by a magnetic field., J Magn Magn. Mater., 1993,122, 335–339.
- [8] N.M Pope, R.C Alsop., Y.A Chang., A.K Smith., Evaluation of magnetic alginate beads as a solid support for positive selection of CD³⁴⁺ cells, J. Biomed. Mat. Res,1994, 2, 449–457.
- [9] M.R Zachariah., M.I Aquino., R.D Shull., E.B Steel., Formation of super paramagnetic nano composites from vapor phase condensation in a flame, Nanostruct. Materials, 1995,5, 383-392.
- [10] Vasant Naidu, et al , Magnetic properties of Nickel, Samarium doped Zinc ferrite, Int. J.Com.App vol 24, 2 (18-22) 2011.
- [11] Vasant Naidu, S.K.A.Ahamed Kandu Sahib, M.Suganthi, ChandraPrakash; Study of Electrical and Magnetic properties in Nano sized Ce-Gd Doped Magnesium Ferrite, Int.J.Com.App vol 27, 5(40-45) 2011
- [12] S. F. Mansour “Frequency and Composition Dependence on the Dielectric Properties for Mg-Zn Ferrite”. Egypt. J. Solids, Vol. (28), No. (2), (2005)
- [13] G.M Bhongale., D.K Kulkarni., V.B Sapre. Determination of cation distribution in spinels, Bull, Mater.Sci.15 (1992)121.
- [14] A Pradeep.,P Priyadharsini., G Chandrasekaran., Sol-gel route of synthesis of nano particles of MgFe₂O₄ and XRD,FTIR and VSM study, Journal of Magn Mag.Mater, 320 (2008) 2779.
- [15] Milen Gateshki et al., Structure of nanocrystallineMgFe₂O₄ from X-ray diffraction, Rietveld and atomic pair distribution function analysis, J. Appl. Cryst. (2005). 38, 772–779/
- [16] M.Z Said., D.M Hemed., S.A Kader., and G.Z Farag., Turk, “Structural, electrical and infrared studies of Ni_{0.7}Cu_{0.3}Zn_xFe_{2-x}O₄ “J. Phys., 2007, 31: 41.
- [17] R. R. Heikes and D. Johnston, The Preparation and Magnetic Properties of High Purity Raney Iron J. Chem. Phys. 26, 582 (1957).
- [18] B.D Cullity., Elements of X-Ray Diffraction, Addison Wesley Pub. Co. Inc., London 1967: 96.
- [19] A.A Sattar., et.al, Rare Earth Doping Effect on the Electrical Properties of Cu-Zn Ferrites, [J] J. Phys. IV France 1997, 7.
- [20] A.B Gadkari., T.J Shinde., and P.N Vasambekar., Structural analysis of Y³⁺ doped Mg-Cd ferrites prepared by oxalate co-precipitation method, J. Mater. Chem. Phys., 2009, 114 (2-3): 505.
- [21] R.D Waldron., Infrared spectroscopy of ferrites, Phy. Rev., 1955, 99: 1727.
- [22] O.M Hemed., IR spectral studies of Co_{0.6}Zn_{0.4}Mn_xFe_{2-x}O₄ ferrites, J. Magn. Mater., 2006, 281: 36.
- [23] Vasant Naidu, S.K.A.AhamedKanduSahib, M.SheikDawood, M.Suganthi; Magnetic Properties of Nano Crystalline Nickel, Cerium doped Zinc Ferrite , Int.J.Nano tech and Nano Sci in press.
- [24] N Rezlescu., ERezlescu., C Pasnicu., and M.L Craus., Effect of the rare-earth ions on some properties of nickel-zinc ferrite, J. Phys. Condens. Matter, 1994, 6: 5707.

- [25] X Liu., W Zhong., S Yang., Z Yu., B Gu., and Y Du., Influence of La^{3+} substitution on the structural and magnetic properties of M-type strontium ferrites, *J. Magn. Mater.*, 2002, 238 (2-3): 207.
- [26] L Gama., A.P Dlniz., A.C.F.M Coasta., S.M Rezend., A Azevedo., and D.R Cornejo., Magnetic properties of Ni-Zn ferrite doped with samarium, *Phys. B*, 2006, 384 (1-2): 97
- [27] M.S. Mattsson, G.A. Niklasson, K. Forsgren, A. Harsta,” A frequency response and transient current study of β - Ta_2O_5 : Methods of estimating the dielectric constant, direct current conductivity, and ion mobility” *J. Appl.Phys.* 85 (4) (1999) 2185.
- [28] Vasant Naidu, et.al, “Synthesis of Nano sized Sm-Gd doped Magnesium ferrite and their Permittivity and Hysteresis Studies”, *Int. J.Com.App*, vol 30(7), (13-23) 2011.